J Mater Sci (2007) 42:6578–6582
DOI 10.1007/s10853-007-1511-3

Superplastic behavior of an extruded eutectic NiAl/Cr(Mo) alloy at intermediate strain rate region

Du Xinghao · Wu Baolin · C. J. Lee · J. C. Huang

Received: 1 January 2006 / Accepted: 9 January 2007 / Published online: 30 April 2007

Abstract The superplastic behavior of cast and hot-extruded NiAl–28Cr–6Mo is observed in the strain rates between $\dot{\varepsilon} = 1.04 \times 10^{-3}$ and 5.02×10^{-2} s^{-1} at 1323–1373 K. The synchronous operation of dislocation glide and dynamic recovery is responsible for the tested alloy to exhibit superplastic behavior.

Introduction

The B2-type intermetallic compound NiAl is an attractive matrix to replace nickel-based superalloys for high temperature structural materials due to its high melting point, low density, good thermal conductivity and good oxidation resistance [1, 2]. However, poor damage tolerance at ambient temperatures and inadequate strength at high temperatures have prevented its commercial applications. It has reported that these shortcomings can be improved significantly by the fabrication of NiAl-based eutectic composites involving a refractory metal reinforcement phase, and NiAl/Cr(Mo) alloys display the promising mechanical properties [3, 4]. These materials, however, are difficult to form by conventional processing routes due to high melting points and poor machinability from the high elastic modulus. Fortunately, it is known that superplasticity can provide the possibility for high-temperature deformation processing of these brittle materials, and has the advantages of sharper formability with better dimension accuracy [5].

It is known that superplastic behavior can occur at strain rates of, typically, ~10^{-4} s^{-1} to 10^{-3} s^{-1}. Obviously, these low rates are unacceptable in practice. However, if the strain rates for superplastic deformation are ~10^{-3} s^{-1} to 10^{-2} s^{-1}, the production time by superplastic forming is of the order of ~20–30 min, which is acceptable for the fabrication of high-value components with highly specialized applications, as in aircraft [6]. On this basis, the deformation behavior and mechanism of an extruded eutectic NiAl–28Cr–6Mo alloy for strain rates of ~$10^{-3}s^{-1}$ to $10^{-2}s^{-1}$ are investigated in this present study.

Experimental procedure

The nominal NiAl–28Cr–6 Mo (at.%) alloy, prepared from high-purity metals as starting materials, was vacuum induction melted and drop cast into a cylindrical chill mold. The master alloy was homogenized at 1300°C for 24 h. Afterwards, the alloy was extruded with an area reduction 9:1 at 1000°C. The flat tensile specimens, with a gauge section of $2 \times 2.5 \times 16$ mm^3, were electro-discharge machined from as-extruded material. Tensile tests were performed using a SHIMADZU AG-25KNE testing machine up to 1373 K. Tensile specimens were heated to the deformation temperature at a heating rate of 15 K/min and maintained at the temperature with an accuracy of ±1 K during deformation under constant crosshead speed conditions. By subtracting difference between the recorded displacement data with the measured specimen length, the

D. Xinghao · C. J. Lee · J. C. Huang (✉)
Institute of Materials Science and Engineering, Center for Nanoscience and Nanotechnology, National Sun Yat-San University, Kaohsiung 804, Taiwan, ROC
e-mail: jacobc@mail.nsysu.edu.tw

D. Xinghao · W. Baolin
Department of Materials Engineering, Shenyang Institute of Aeronautical Engineering, Shenyang 110034, P.R. China

displacement data were corrected to allow for test machine compliance. The true strain is calculated by the equation of $\varepsilon = \ln(1+\delta)$, where δ is the engineering strain. The initial strain rate is calculated by the equation of $\dot{\varepsilon} = \frac{v}{L}$, where v is the cross head speed and L is the original gage length of the specimen. The specimens were pulled isothermally at a constant cross head speed, which ranged from 0.1 mm/min to 10 mm/min, corresponding to initial strain rate of 1.04×10^{-4} to a strain rate of 1.04×10^{-2} s^{-1}, until final fracture occurred. Tensile loads were automatically recorded through a supplementary computer, true stress–true strain curves were drawn from data recorded by the computer under the assumption of volume constancy.

To investigate the microstructural changes, some specimens were deformed to a prescribed strain, then unloaded and water-quenched. The specimens for scanning electron microscopy were etched in a solution of 5 g $FeCl_3$ + 15 ml HCl + 65 ml CH_3COOH. Thin foils for TEM observation were taken from the center part of the gage section and prepared by argon ion milling after mechanical polishing to 30 μm. The electron-transparent samples were subsequently examined in a Philips EM 420 analytical electron microscope operated at 120 kV.

Experimental results

The tensile properties

Figure 1 shows the macrograph of the fractured NiAl–28Cr–6Mo specimens tested in tension at 1323–1373 K and initial strain rate range of 1.04×10^{-3}–1.04×10^{-2} s^{-1}, which shows that the tensile elongations all are beyond the value of 300%. And the elongation increases with the increase of tested temperature.

The true stress–true strain curves

True stress–true strain curves are drawn from data recorded by the computer according to the method employed by Oomori et al. [7]. This method makes an assumption of uniform deformation over the gage section of specimen during the superplastic deformation process. From Fig. 1, we know that the assumption is acceptable. Because the volume of gage section is constant, and it is the product of length and cross-section area of the gage section, the instantaneous area of gage section can be obtained for the specimen during deformation process. By dividing the instantaneous load by the instantaneous area of section, the true stress can be obtained. Since all the tests are conducted with constant crosshead speed, the curves of flow stress versus strain may be somewhat different from those under the condition of constant strain rate.

Fig. 1 Macrographs of fracture specimens of NiAl–28Cr–6 Mo alloy

Based on the stress versus strain relationship in superplasticity, $\sigma = K\dot{\varepsilon}^m$; where k is a constant, a correlation to transform the stress at non-constant strain rate to that at constant strain rate is developed as

$$\sigma_{c\varepsilon} = \sigma_{cv} e^{m(\varepsilon - 0.002)} \quad (1)$$

$\sigma_{c\varepsilon}$ constant strain rate, 0.002 is true strain corresponding to yielding point, σ_{cv} is the stress under the condition of constant cross head speed. According to the above correlation, the curves of flow stress versus strain were re-plotted in Fig. 2. From Fig. 2, we can observe that at 1323 K under the initial strain rate of $5.20 \times 10^{-3}s^{-1}$, the true stress–true strain curve under the constant strain rate exhibits pronounced increase after yield, followed by rapid decrease of stress.

Constitutive equation

High temperature deformation of materials under steady-state conditions can be generally expressed by the relation between flow stress (σ) and strain rate ($\dot{\varepsilon}$):

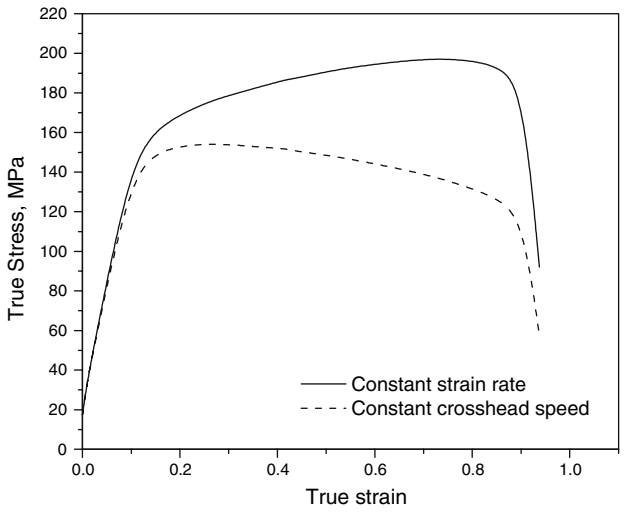

Fig. 2 True stress–true strain curves for the tested alloy under the initial strain rate of $5.20 \times 10^{-3}s^{-1}$

$$\dot{\varepsilon} = A\sigma^{n} \exp(-Q/RT) \quad (2)$$

where A is a constant, n is the stress exponent being identical to $1/m$ (m is the strain rate sensitivity index), Q is the apparent activation energy, R is a gas constant and T is the thermodynamic temperature [8]. Figure 3 shows the relationship between the flow stress and the strain rate for the tested alloy at various temperatures. Figure 3a shows the strain rate sensitivity index $m \approx 0.33$ for the alloy at 1323 K and 1373 K under the strain rate of $10^{-3}s^{-1}$–$10^{-2}s^{-1}$.

From Eq. 1 it can be shown that:

$$Q = n \cdot R \cdot \frac{\partial \ln \sigma}{\partial(1/T)} \quad (3)$$

where $n = 1/m$. Figure 3b shows an Arrhenius plot for the flow stress of the tested alloy where the stresses corresponding to the steady flow in the true stress–true strain curves were used as the flow stress. The plot was obtained for strain rates of $5.20 \times 10^{-3}s^{-1}$ ($n = 3$). The apparent activation energy is calculated to be about 305 kJ/mol based on the Eq. 2, which is about equal to the value (250–300 kJ/mol) measured in creep deformation of NiAl [1].

Microstructural observation

An SEM image showing a typical microstructure of the alloy obtained after hot extrusion is shown in Fig. 4a. The NiAl-matrix grains (gray color) are equiaxed and fine. The linear intercept grain size is determined as 3–5 μm. A club-shaped Cr(Mo) phase (white color) is distributed along the extrusion direction. Figure 4b shows the SEM image of the specimen after a strain of 0.8 at 1323 K under an initial strain rate of 5.20×10^{-3} s^{-1}. The grains of primary β-NiAl matrix in the gage section have significantly coarsened, with the mean grain size of more than 10 μm. The elongated Cr(Mo) phase has been replaced by a more homogeneous microstructure and the agglomeration has occurred.

TEM observations

Figure 5 contains TEM micrographs of the specimens obtained at different strains corresponding to the deformation process at 1323 K under an initial strain rate of 5.20×10^{-3} s^{-1}. A high density of dislocations is visible in Fig. 5a, which illustrates the tendency to form dislocations tangles, as shown at site ''A''. Dislocation networks can be

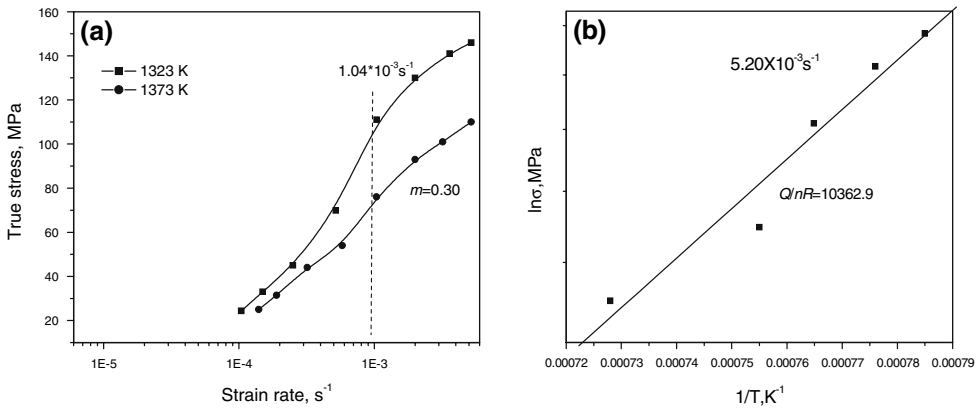

Fig. 3 The Strain rate dependence of true stress (**a**) and Arrhenius plot for the tested alloy

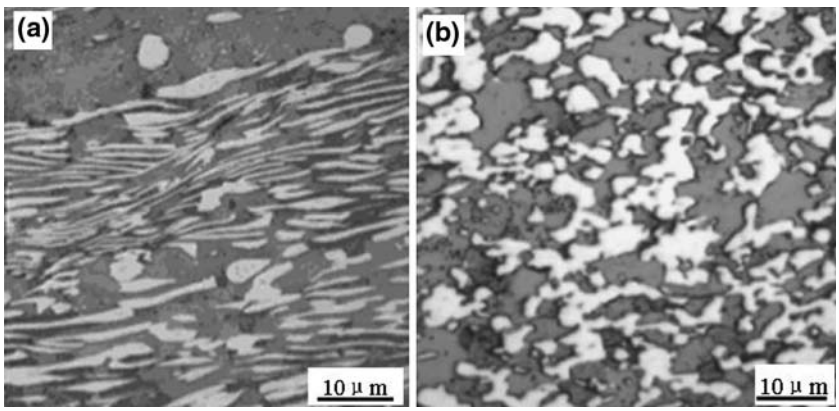

Fig. 4 The SEM images of the specimens for (**a**) $\varepsilon = 0$ (as-extruded); and (**b**) $\varepsilon = 0.8$ at 1323 K under an initial strain rate of 5.20×10^{-3} s^{-1}

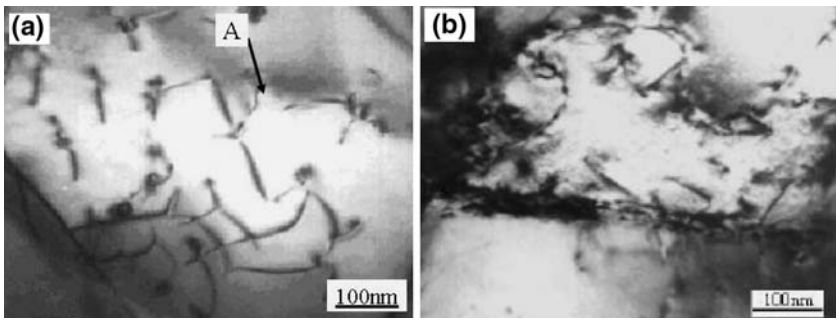

Fig. 5 TEM micrographs of the specimens strained to different values: (**a**) $\varepsilon = 0.20$; (**b**) $\varepsilon = 0.8$ at 1323 K under an initial strain rate of 5.20×10^{-3} s^{-1}

observed in the specimens with the high strains, as shown in Fig. 5b.

Discussion

From foregoing observations, we can conclude that although the high tensile elongations exhibiting at the tested conditions, the deformation characterizes of the alloy do not satisfy the criteria for classical superplasticity of polycrystals due to the low value of m and high apparent activation energy [9]. Jiang et al studied the NiAl/Cr(Mo) alloy with grain size of 10 μm fabricated by hot pressing, and the stress exponent n and activation energy are similar to the present study [10]. Therefore, it is reasonable to conclude that a new mechanism based on grain boundary sliding (GBS) is responsible for the large elongations of the alloy.

TEM examinations show that the dislocation behavior is very active in the grains during the deformation process for the alloy. The phenomenon manifests that slide and multiplication of dislocation are dominant and contribute to a large part of the strain. Furthermore, with the increase of strain (Fig. 5b) the appearance of clearly discernible subgrain boundaries indicates that restoration process has occurred. It is generally believed that in ordered intermetallics, dislocations glide in the form of superdislocations, i.e. a pair of unit dislocations connected with planar fault. It is well known that the high stacking fault energy of B2 NiAl urges the activated dislocation to shrink and climb instead of splitting into partials at elevated process [1, 2]. Thus, dynamic recovery occurs rather than competing process of conventional dynamic recrystallization. From Fig. 5c, the appearance of the dislocations observed in Fig. 5c suggests that dislocation climb is occurring during the deformation process. The value of $Q = 305$ kJ/mol can be interpreted in terms of high temperature dislocation climb as a controlling process for the deformation. This type of dislocation climb is controlled by vacancy diffusion along dislocation cores and may cause dislocation rearrangement at small distances [11]. In addition, the high diffusion rate of B2 NiAl enables fast vacancy migration, and thus promotes the dynamic recovery (DR) process [1, 2]. The DR process can reduce internal stress and promote further dislocation motion in addition to accommodating grain compatibility in NiAl.

On the other hand, the high tensile elongation of extruded NiAl polycrystals at high temperatures occurs concurrently with pronounced strain hardening (see the curve of constant strain rate in Fig. 2). The strain hardening is needed because the onset of localized deformation (necking instablility) in tension is governed by the Considére criterion [12, 13]:

$$\left(\frac{\partial\sigma}{\partial\varepsilon}\right) \leq \sigma \tag{4}$$

where σ and ε are true stress and true strain, respectively. In this test, the tested alloy tended to increase the work hardening (left-hand side of Eq. 4) quickly on deformation owing to their high dislocation storage efficiency inside the NiAl grains even in the presence of DR. The work hardening arises from both the substitution effects of the elements of Cr, Mo and vacancy. Accordingly, the synchronous operation of dislocation glide and dynamic recovery is responsible for the tested alloy to exhibit large elongations.

It should be noted that similar phenomena have been observed in FeAl, Fe_3Al, and Fe_3Si alloys [14–17]. The common characteristics of them are that the values of m (about 0.30) and fracture elongations are not very high. But the elongation beyond 300% is sufficient to make, using superplastic forming technology, extremely complex shapes for most alloys, which only require over 300% elongation [9]. In this paper, because the NiAl alloy exhibits large elongation behavior under the strain rate of the order of ~10^{-3} s^{-1} to 10^{-2} s^{-1}, there is great interest in using the material for engineering structures.

Conclusions

1 The cast and hot-extruded NiAl–28Cr–6Mo alloy exhibits large tensile elongation, greater than 300%, for

strain rates of 1.04×10^{-3} and 5.02×10^{-2} at temperatures of 1323 K and 1373 K, respectively.

2 The synchronous operation of dislocation glide and dynamic recovery is responsible for the alloy to exhibit large elongations.

Acknowledgements The authors would like to acknowledge the projects (05YB31) supported by the scientific research initial foundation for doctor of Shenyang Institute of Aeronautical Engineering.

References

1. Miracle DB (1993) Acta Metall Mater 41:649
2. Noebe RD, Bowman RR, Nathal MV (1994) NASA technical paper, April:3398
3. Johnson DR, Chen XF, Oliver BF, Noebe RD, Whittenberger JD (1995) Intermetallics 3:99
4. Johnson DR, Chen XF, Oliver BF, Noebe RD, Whittenberger JD (1995) Intermetallics 3:493
5. Sakka Y, Matsumoto T, Suzuki TS, Morita K, Kim B-N, Hiraga K, Moriyoshi Y (2003) Adv Eng Mater 5(3):130
6. Langdon TG (1999) Mater Trans JIM 40(8):716
7. Oomori T, Yoneyama T, Oikama H (1988) Trans JIM 29:399
8. Guha S, Baker I, Munroe PR, Michael JR (1992) Mater Sci Eng A 152:2588
9. Sherby OD, Wadsorth J (1989) Prog Mater ScI 33:169
10. Jiang DT, Guo JT, Zhou LZ (1998) Mater Sci Eng 255A:154
11. Griffiths P, Hammond C (1972) Acta Metall 12:935
12. Hart EW (1967) Acta Metall 15:351
13. Jia D (2001) Appl Phys Lett 79:611
14. Lin D, Hu J, Jiang D (2005) Intermetallics 13:343
15. Lin TL, Shan AD, Li DQ Scripta Metall Mater 31:1455
16. Hu J, Lin D (2004) Mater Lett 58:1297
17. Kim WY, Hanada S (1997) Mater Sci Eng A 248A:78